Volume 12, Number 5 (October 2019) p. 1034 – 1057 • ISSN 1983-4195
http://dx.doi.org/10.1590/S1983-41952019000500005

REVISTA IBRACON DE ESTRUTURAS E MATERIAIS
IBRACON STRUCTURES AND MATERIALS JOURNAL

Floors number influence on the instability parameter of reinforced concrete frame-braced buildings

Influência do número de pavimentos no parâmetro de instabilidade de edifícios contraventados por pórticos de concreto armado

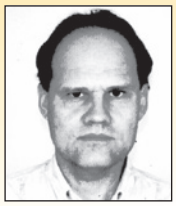

R. J. ELLWANGER [a]
ronaldellwanger@gmail.com
https://orcid.org/0000-0002-5761-5167

Abstract

This work aims to investigate the floors number influence on the instability parameter limit α_1 of reinforced concrete frame-braced buildings; it succeeds another work in this field of knowledge, in which the same question was investigated for wall- and core-braced buildings. Initially, it is showed how the ABNT NBR 6118:2014 (Brazilian code for concrete structures design) defines when a second order analysis is needed. Topics concerning to physical nonlinearity consideration and to the lateral deflection components of frames are also presented. It follows an analytical study that led to the derivation of a method for determining the limit α_1 as a function of the floors number and the relation between bending and shear stiffness. Finally, some examples are presented and their results are used for checking the method accuracy.

Keywords: instability, bracing structures, second order analysis.

Resumo

Este trabalho investiga a influência do número de pavimentos no limite α_1 do parâmetro de instabilidade de edifícios contraventados por pórticos de concreto armado; trata-se da seqüência de uma linha de estudos, na qual esta mesma questão foi investigada em edifícios contraventados por paredes e/ou núcleos. Inicialmente, mostra-se como a ABNT NBR 6118:2014 (norma de projeto de estruturas de concreto) define a necessidade ou não de se realizar uma análise de segunda ordem. Apresentam-se também tópicos relativos à consideração da não linearidade física e às componentes da deformação lateral dos pórticos. Segue-se um estudo analítico que resultou num método de determinação do limite α_1 em função do número de andares e da relação entre as rigidezes à flexão e ao corte. Na seqüência, são apresentados exemplos cujos resultados servem para aferir o grau de precisão do método investigado.

Palavras-chave: instabilidade, estruturas de contraventamento, análise segunda ordem.

[a] *Universidade Federal do Rio Grande do Sul, Departamento de Engenharia Civil, Porto Alegre, RS, Brasil.*

Received: 15 Mar 2018 • Accepted: 18 May 2018 • Available Online:

1. Introduction

1.1 Second order effects and the instability parameter

When acting simultaneously on a building bracing structure, gravity and wind loads can induce additional effects to those usually obtained in a linear or first order analysis. They are the second order effects, in whose computation (second order analysis) the material nonlinear behavior and the structure deflected shape (physical and geometric nonlinearities) must be considered.

Ellwanger [1] and Ellwanger [2] give a summary of the development of tall buildings stability analysis theory and practice, based on the Beck and König discrete model, shown in figure 1. In this model, with equally spaced floors, all bracing substructures are grouped in a single column, while all braced elements (bearing elements that don't belong to the bracing system) are replaced by an assemblage of hinged bars. *W* denotes the wind load applied on each floor, while *P* and *V* are the floor vertical loads, applied on the bracing substructures and braced elements, respectively. The loads *W*, *P* and *V* are considered with their characteristic values.

The above mentioned articles also show that, in order to compute the global bending moments on the building structure, including second order effects, the vertical loads acting on the bracing system are given by its own *P* loads added to the braced elements *V* loads.

The development of the above mentioned stability analysis theory originates a constant α, as a function of the building height, its total vertical load and the bracing system horizontal stiffness. This constant is defined as the instability parameter, being expressed by equation (1). Another contribution of the aforesaid theory was to define a criterion according to that the second order effects may be neglected, provided that they don't represent an increase more than 10% on the first order effects. When applying this criterion to the global bending moment at the bracing system support, the instability parameter becomes limited to particular values.

The present Brazilian code for concrete structures design (ABNT NBR6118:2014, ABNT [3]) adopted the just mentioned criterion, determining in its section 15 that second order global effects are negligible when lower than 10% of the respective first order effects. In order to verify this possibility, the code presents two approximate procedures, being one of them based on the instability parameter; the code determines that in a symmetrical framed structure the second order effects may be neglected provided that its instability parameter α will be lesser than the value of α_1, according to the expressions:

$$\alpha = H_{tot}\sqrt{N_k/(E_{cs}I_c)} \quad (1)$$

$$\alpha_1 = 0.2 + 0.1n \ \ for \ n \leq 3 \ \ \wedge \ \ \alpha_1 = 0.6 for \ n \geq 4 \quad (2)$$

n is the number of floors above the foundation or a slightly displaceable subsoil level. H_{tot} is the structure height, measured from the same level. N_k is the summation of all vertical loads acting on the structure (along the height H_{tot}), with their characteristic values. $E_{CS}\,I_C$ represents the summation of all columns stiffness values in the bracing direction. I_C is the moment of inertia considering the columns gross sections. E_{CS} is the secant elasticity modulus, expressed by:

$$E_{CS} = rE_{Ci} = (0.8 + 0.0025f_{ck})E_{Ci} \leq E_{Ci} \quad (3)$$

f_{ck} is the concrete compressive characteristic strength. E_{Ci} is the tangent elasticity modulus, being dependent of f_{ck} and the gravel material, according to the equations presented by item 8.2.8 of ABNT [3]. *r* is a coefficient relating E_{CS} with E_{Ci}; it is expressed by the second equality of equation (3) and is represented by a_i in the code. E_{CS}, E_{Ci} and f_{ck} are given in MPa.

Furthermore, the code determines different α_1 values, depending on the bracing structure type: the limit value $\alpha_1 = 0.6$, prescribed for $n \geq 4$, is generally applicable to building usual structures. It must be adopted for wall-columns assemblages and for rigid frames associated to wall-columns. It has to be increased until 0.7 in the case of bracing systems composed exclusively by wall-columns and must be reduced to 0.5 if there are only rigid frames.

Although not belonging to this work purpose, a mention deserves to be done to a computer aid method, based on the moment amplification factor g_z. Presented in 1991 by Franco and Vasconcelos [4], it also applies the criterion of 10% increase in relation to first order effects, to define if a second order analysis is or not needed. Furthermore, a great variety of powerful structural analysis softwares is nowadays available, allowing an accurate modeling of building structures.

In spite of the disposal of more advanced analysis tools, the instability parameter preserves its importance. On using it, the building structure is modeled as a single column, according to Ellwanger [1]. The utmost simplicity of this model facilitates the understanding of the system global behavior, specially the influence of the system total weight and lateral stiffness on its stability. In this way, the instability parameter has proved to be well fitted for the early stages of design, as the structure initial definition. Furthermore, I_C can be isolated in equation (1), originating a very simple way of determining, at the stage of pre-dimensioning, the minimum horizontal stiffness needed for second order analysis exemption.

In the specialized literature, the instability parameter has been

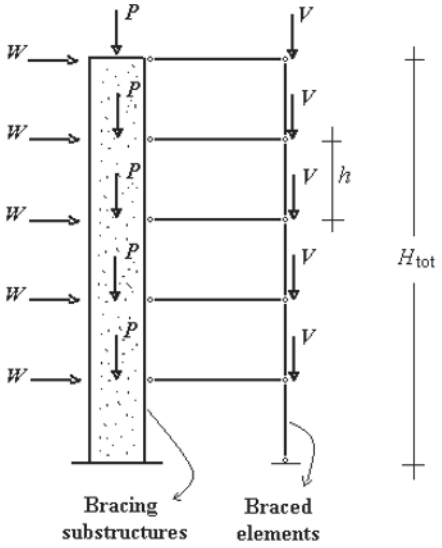

Figure 1
Discrete model of Beck and König

approached in several articles that deal with building structures global stability. Concerning this, some articles may be mentioned, as Alves e Feitosa [5], about structures with prestressed slabs; Cicolin e Figueiredo Filho [6], about structures consisting of slab bands and inverted border beams; and Freitas et ali [7], about the influence of columns compressive stress.

1.2 Reasons and targets of this work

Ellwanger [1] searched a way to define the limit a_1 of the instability parameter of bracing systems formed by assemblages of rigid frames and shear walls or cores, variable with the relation between their horizontal stiffness coefficients. The equation derived for this purpose revealed a good accuracy only for buildings with a great number of floors, resulting in significant errors for less than 30 floors. One of the search conclusions was that the formulation for performing such a prediction had necessarily to take into account the building floors number.

In a subsequent work, Ellwanger [2] searched a way to predict the limit α_1 for buildings braced exclusively by shear walls and cores, variable with the floors number. The investigation led to an equation that provided a very good accuracy for the analyzed examples. Succeeding the studies about this subject, the present work focuses on bracing systems constituted exclusively by rigid frames.

Concerning to the instability parameter as a function of the floors number, ABNT [3] determines variable limits only for buildings with less than four floors. In its turn, the prescription of fixed limits (0.5, 0.6 or 0.7, depending on the bracing structure type) for a greater number of floors is questionable. For example, Ellwanger [1] found differences of about 15 % between the limit coefficients α_1 of a building braced exclusively by rigid frames, with the number of floors varying from 5 until 30. Considering that the instability parameter computation requires a square root extraction, the difference between the corresponding vertical load/horizontal stiffness ratios reaches 32 %. Consequently, on verifying the exemption of performing a second order analysis, the error on determining the required horizontal stiffness can become significant.

This work aims to research a way of defining the instability parameter limit α_1 for buildings braced by rigid frames, variable with the number of floors. At first, topics concerning to physical nonlinearity consideration and to the lateral deflection components of frames are presented. These topics are useful for the next section of the work, in which a computer aid method, based on the discrete model of Beck and König, shown in figure 1, is developed in order to determine the α_1 limits for buildings with any number of floors. The method is then applied for a sequence of floors numbers, generating various series of α_1 values, which are arranged in tables. Thereafter, the accuracy of these values is checked in two examples of buildings braced by rigid frames; 10 tests are performed, with the number of floors varying from 5 until 50.

2. Consideration of physical nonlinearity

In a second order analysis, the effects of both physical and geometric nonlinearities must be considered. In its item 15.7.3, the ABNT NBR 6118:2014 code allows to consider the physical nonlinearity in an approximated manner. This is done by means of a reduction of the structural members stiffness factors $(EI)_{sec}$ in function of $E_{Ci} I_C$, or of $E_{CS} I_C$ if equation (3) is used. Although the code restricts this procedure to four or more floors structures, in this work it will also be adopted for buildings with three or less floors. Therefore, this fact must be kept in mind when results of examples with few floors are analyzed. Considering r as defined by equation (3) and representing the tensile and compressive longitudinal reinforcement areas respectively by A_s and A_s', it may be written:

- beams:

$$(EI)_{sec} = 0.4E_{Ci}I_C = 0.4E_{CS}I_C/r \quad (A_s \neq A_s') \tag{4}$$

$$(EI)_{sec} = 0.5E_{Ci}I_C = 0.5E_{CS}I_C/r \quad (A_s = A_s') \tag{5}$$

- columns:

$$(EI)_{sec} = 0.8E_{Ci}I_C = 0.8E_{CS}I_C/r \tag{6}$$

This study requires the determination of the ratio $(EI)_{sec}/E_{CS}I_C$ of the rigid frame members assemblage. It is in fact a merely representative value, because this relation cannot be considered constant, since it can vary in function of many factors, as the number and height of stories, number and length of spans, relation between the dimensions of beams and columns cross sections etc. Pinto and Ramalho [8] proved that the physical nonlinearity influence on rigid frames lateral stiffness relies mainly on the loading magnitude and reinforcement rates, having obtained relations $(EI)_{sec}/E_{CS}I_C$ varying from 0.51 to 0.75.

Taranath [9] states that the shear mode of deformation accounts for up to 80% of the total sway of a rigid frame, being 60% due to beam flexure and 20% due to column bending. The cantilever deflection due to column axial deformations accounts for up to 20%; in its turn, Smith and Coull [10] asserts that this contribution is usually less than 10% of the shear deformation, except in very tall and slender rigid frames. Due to these considerations, in the subsequent study, the contribution of beams and columns flexibility for the total sway of a rigid frame will be assumed as 65% and 35%, respectively.

In a slender frame, the beam reinforcements A_s and A_s' tend to be the same, due to the predominance of wind effects. Thus, in this case, equations (5) and (6) may be employed to relate the contributions of beams and columns flexibility for the horizontal displacements, resulting from physical nonlinear analysis, with the corresponding contributions resulting from linear analysis. At the same time, applying the above mentioned proportions of 65% and 35% of these contributions for the total horizontal displacements and performing the same algebraic transformations presented in section 4 of Ellwanger [1], it can be proved that:

$$(EI)_{sec} = 0.5755E_{CS}I_C/r \tag{7}$$

3. Lateral distortion components of a rigid frame

In bracing substructures of the rigid frame type, the deflections due to bending of the individual beam and column members are predominant. When the frame is subject to horizontal loads, the global bending moment is mainly carried to the columns as axial forces, for which the structure has a high stiffness. Thus, the frame horizontal deflections are mostly caused by global shear.

Furthermore, there exists another factor inducing lateral distortions, whose importance increases with the frame height and slenderness. This factor is related to the just mentioned global bending moment and consists of column axial deformations, inducing bending of the frame as a whole. Thus, according to Taranath [9], rigid frames can be modeled as vertical cantilever bars in which bending and shear distortions occur simultaneously.

Figure 2-a shows a rigid plane frame subject to a uniform horizontal load of ratio *w*, as well as a vertical bar with a constant cross section, equivalent to the frame; the horizontal displacements *y(x)* of the bar axis points and its derivatives $\phi(x)$ can be expressed by the sum of the components due to bending and shear effects, denoted by sub-indexes *F* and *C*, respectively:

$$y(x) = y_F(x) + y_C(x) \tag{8}$$

$$\phi(x) = \phi_F(x) + \phi_C(x) \tag{9}$$

The component $\phi_F(x)$ corresponds to the bar cross sections rotations induced by bending, while $\phi_C(x)$ represents the deflected shape slope due to shear. The bar behavior under bending is expressed by:

$$EJ\, d^2y_F/dx^2 = -M(x) = w(\ell - x)^2/2 \tag{10}$$

ℓ is the bar length, *E* is the material longitudinal elasticity modulus and *M(x)* is the global bending moment, considered negative when inducing tension on the bar left side; *J* is the bar cross section moment of inertia, that can be determined from the cross sections areas of the frame columns and the distances between their axes and the centroid of these areas.

The behavior of the structure under shear will be expressed, making use of a proportionality factor *S* between the global shear force *Q(x)* and the deflected shape slope given by $\phi_C(x)$. Thus, *S* represents the system (plane frame) stiffness to global shear. It is verified that the factor *S* is in fact subjected to variations along the frame height, which are greater next its support. Smith and Coull [10] present an approximate expression for *S* at a generic floor *i* (*i* > 1):

$$S_i = \frac{12E}{h_i(1/G_i + 1/C_i)} \tag{11}$$

h_i is the height of floor *i*. G_i denotes the summation of the ratios *I*/*L*, being *I* the moment of inertia and *L* the length of each beam member of floor *i*; C_i has the same meaning of G_i concerning to the column members. For the first floor, in the case of all the columns being rigidly connected at support, *S* is given by:

$$S_1 = \frac{12E(1 + C_1/6G_1)}{h_1(2/3G_1 + 1/C_1)} \tag{12}$$

The examples presented in section 5 are characterized by keeping the same geometry of beams and columns at all the floors. Thus, applying equations (11) and (12) will give, for each example, a single value of S_i (*i* > 1), besides a value of S_1. In its turn, the relations S_1/S_i, computed for the examples, vary significantly, showing a median value of 2.17. In the present study, in order to simplify the formulation, an experience will be made, adopting a single value for the relation S_1/S_i. The value 2 will be adopted, since it is the hithermost integer to the just mentioned median value. Since it is an approximation based on a mere sample, its effects in the analysis results remains to be estimated, not only for the examples of this work, but also for any other ones in which the present method will be investigated.

In this way, applying the condition of proportionality between *Q(x)* and $\phi_C(x)$, the behavior of the frame equivalent bar, due to shear, may be expressed by:

$$\phi_C(x) = Q(x)/mS = w(\ell - x)/mS \tag{13}$$

Considering that was explained in the penultimate paragraph, *m* will be considered equal to 2 for the first floor and equal to unity for the remaining ones. Integrating (10) and (13), applying the appropriate boundary and continuity conditions, leads to the functions $y_F(x)$ and $y_C(x)$. Replacing them into (8) determines *y*(*x*); applying this function for $x = \ell$, gives:

$$\Delta_T = y(\ell) = \frac{w\ell^4}{8EJ} + \frac{w\ell^4 N}{4S\ell^2} \tag{14}$$

where

$$N = 1 + (1 - 1/n)^2 \tag{15}$$

In its turn, figure 2-b shows a vertical cantilever bar that is also equivalent to the rigid frame of figure 2-a. It is subject to the same loading, but in this case the distortion due to shear is neglected. Representing by *I* the moment of inertia of the bar cross section, the top horizontal displacement will be given by:

$$\overline{\Delta}_T = \bar{y}(\ell) = w\ell^4/8EI \tag{16}$$

On dealing with the instability parameter, item 15.5.2 of ABNT NBR 6118:2014 code determines a procedure for evaluating the $E_{CS}I_C$ stiffness factor of a constant cross section column, equivalent to a given rigid frame. According to this procedure, this stiffness factor should be obtained computing initially the horizontal displacement on the bracing structure (frame) top, under the horizontal loading, which is just D_T given by equation (14). The next step is to obtain the stiffness factor of an equivalent column with constant cross section such that, under the same loading, undergoes the same top horizontal displacement which, in this case, is $\overline{\Delta}_T$ given by

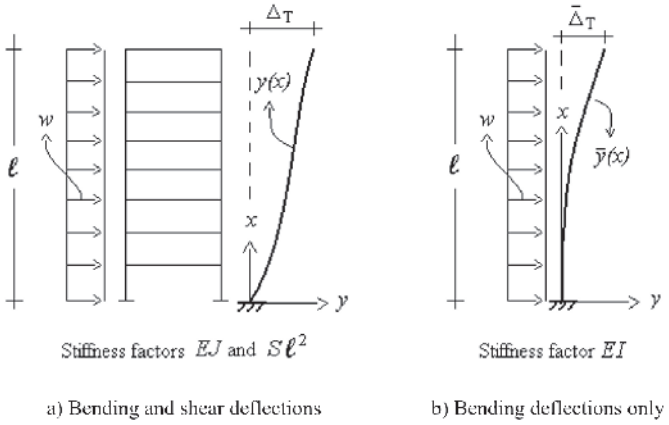

Figure 2
Columns equivalent to a rigid plane frame

(16). This implies in equality between these expressions, resulting:

$$S\ell^2 = \frac{2N\,EIJ}{J-I} \tag{17}$$

4 . Second order effects on the discrete model

According to the Beck and König model, described in subsection 1.1, a bracing system composed by rigid frames may be modeled by a simple bar, behaving as a column. Figure 3 shows a cantilever bar of length H_{tot}, modeling the bracing system of a building with n floors of the same height h. It is subject to gravity loads F (given by the sum of actions P and V of figure 1) and wind loads (W/2 at top and W on the remaining floors). The loads are considered with their characteristic values. The bar has a constant moment of inertia J along its length; the stiffness to shear is 2S on interval n and S on the remaining ones.

4.1 Interaction between successive bar intervals

Taking the bar deflections into account (geometric nonlinearity), the behavior of a generic interval i under shear is expressed by:

$$mS\phi_{Ci}(x) = Q_i(x) = W(i-1/2) + iF\phi_i(x) \tag{18}$$

Applying equation (9) for interval i, replacing it into (18) and isolating $\phi_{Fi}(x)$, results:

$$\phi_{Fi}(x) = (1 - iF/mS)\phi_i(x) - (W/mS)(i-1/2) \tag{19}$$

Deriving equation (19) in relation to x, gives:

$$d\phi_{Fi}/dx = d^2y_{Fi}/dx^2 = (1 - iF/mS)d^2y_i/dx^2 \tag{20}$$

The behavior of the same interval i under bending is expressed by:

$$EJ\, d^2y_{Fi}/dx^2 = -M_i(x) \tag{21}$$

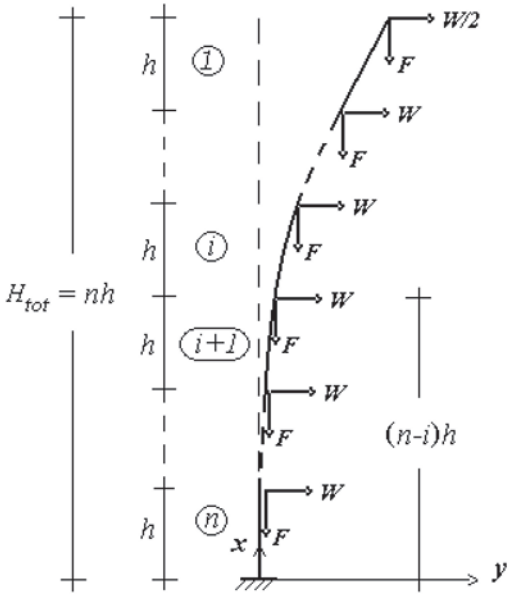

Figure 3
Column equivalent to a bracing system with n floors

Introducing (20) into (21) and expressing $M_i(x)$ in function of the loads, results:

$$EJ(1 - iF/mS)d^2y_i/dx^2 = W\left\{(nh - x)/2 + \sum_{j=1}^{i-1}[(n-j)h - x]\right\} - F\left\{iy_i(x) - \sum_{j=0}^{i-1} y_{i+1}[(n-j)h]\right\} \tag{22}$$

The solution of (22) and its derivative are given by:

$$y_i(x) = \frac{1}{i}\sum_{j=0}^{i-1} y_{i+1}[(n-j)h] + C_{2i-1}sen(\sqrt{i}a_i x) + C_{2i}cos(\sqrt{i}a_i x) + \frac{W}{iF}\left\{\frac{nh-x}{2} + \sum_{j=1}^{i-1}[(n-j)h - x]\right\} \tag{23}$$

$$\frac{dy_i}{dx} = \phi_i(x) = \sqrt{i}a_i\left[C_{2i-1}cos(\sqrt{i}a_i x) - C_{2i}sen(\sqrt{i}a_i x)\right] - \frac{W}{iF}\left(i - \frac{1}{2}\right) \tag{24}$$

C_{2i-1} and C_{2i} are integration constants and the coefficient a_i is given by:

$$a_1^2 = F/EJ(1 - iF/mS) \tag{25}$$

Applying equation (23) for the system top ($x = nh$ and $i = 1$), gives:

$$C_2 = -C_1 \tan(na_1 h) \tag{26}$$

Having a relation between C_1 and C_2 been obtained, it will now be shown how the integration constants concerning to a given bar interval can be expressed in function of the constants regarding to the preceding one. The function $y_{i+1}(x)$ is obtained, replacing i by $i + 1$ in equation (23). Then, expressing successively $y_i(x)$ and $y_{i+1}(x)$ for $x = (n - i)h$ (transition between intervals i and $i + 1$) and performing the same algebraic transformations presented by Ellwanger [2], it can be proved that:

$$C_{2i+1}sen\left[\sqrt{i+1}(n-i)a_{i+1}h\right] + C_{2i+2}cos\left[\sqrt{i+1}(n-i)a_{i+1}h\right] = B_1 \tag{27}$$

where

$$B_1 = \frac{i}{i+1}\left\{C_{2i-1}sen\left[\sqrt{i}(n-i)a_i h\right] + C_{2i}cos\left[\sqrt{i}(n-i)a_i h\right]\right\} \tag{28}$$

At the transition between two generic bar intervals, the sudden change of shear force causes a discontinuity in the component $\phi_C(x)$ of the bar deflected shape slope; in its turn, the components $\phi_F(x)$ at the end of an interval and at the beginning of the following one are the same. Replacing (24) into (19), gives:

$$\phi_{Fi}(x) = \left(1 - \frac{iF}{mS}\right)\sqrt{i}a_i\left[C_{2i-1}\cos(\sqrt{i}a_i x) - C_{2i}sen(\sqrt{i}a_i x)\right] - \frac{W}{iF}\left(i - \frac{1}{2}\right) \tag{29}$$

Replacing i by $i + 1$ in equation (29) determines $\phi_{F,i+1}(x)$. The condition of ϕ_F continuity implies in equality between the functions $\phi_{Fi}(x)$ and $\phi_{F,i+1}(x)$ for $x = (n - i)h$, resulting:

$$C_{2i+1}cos\left[\sqrt{i+1}(n-i)a_{i+1}h\right] - C_{2i+2}sen\left[\sqrt{i+1}(n-i)a_{i+1}h\right] = B_2 \tag{30}$$

where

$$B_2 = \frac{\sqrt{i}}{\sqrt{i+1}}\frac{\sqrt{1 - iF/mS}}{\sqrt{1 - (i+1)F/mS}}\left\{\begin{matrix} C_{2i-1}cos\left[\sqrt{i}(n-i)a_i h\right] - \\ C_{2i}sen\left[\sqrt{i}(n-i)a_i h\right] \end{matrix}\right\} + \frac{Wh}{2i(i+1)^{3/2}a_{i+1}hF[1 - (i+1)F/mS]} \tag{31}$$

Modifying equations (27), (28), (30) and (31) adequately, C_{2i+1} and C_{2i+2} become expressed in function of C_{2i-1} and C_{2i}, as follows:

$$C_{2i+1} = B_2 cos\left[\sqrt{i+1}(n-i)a_{i+1}h\right] + B_1 sen\left[\sqrt{i+1}(n-i)a_{i+1}h\right] \quad (32)$$

$$C_{2i+2} = B_1 cos\left[\sqrt{i+1}(n-i)a_{i+1}h\right] - B_2 sen\left[\sqrt{i+1}(n-i)a_{i+1}h\right] \quad (33)$$

4.2 Determination and comparison between support bending moments

Having a relation between the integration constants concerning to two successive bar intervals been determined, an expression for the bending moment at the bar support will now be deduced. The condition of null ϕ_F rotation at support is imposed, canceling equation (29) for $x = 0$, $i = n$ (last interval) and $m = 2$. Thereafter, C_{2n-1} can be isolated, giving:

$$C_{2n-1} = \frac{(n-1/2)W}{n\sqrt{n}a_n F(1-nF/2S}} \quad (34)$$

Ellwanger [2] shows that, combining equations (20) and (21) with the derivative of (24), leads to the following expression for the bending moment at support:

$$M(0) = M_n(0) = nFC_{2n} \quad (35)$$

The deduction of the expression of $M(0)$ for buildings with a generic number n of floors starts with the application of equation (26), so that C_2 results expressed in function of C_1. Thus, applying equations (32) and (33) for the transition between the first and second intervals ($i = 1$) determines expressions for C_3 and C_4 having C_1 as the only integration constant. The same will happen to the other constants, when applying those equations for the remaining intervals. Furthermore, due to the last term of the expression of B_2 given by (31), the successive applications of (32) and (33) generate expressions for the integration constants having a term multiplied by Wh/F that is independent of C_1. Hence, this procedure generates expressions for C_{2n-1} and C_{2n} (interval n) that may be put into the form:

$$C_{2n-1} = A_1 C_1 + D_1 Wh/F \quad (36)$$

$$C_{2n} = A_2 C_1 + D_2 Wh/F \quad (37)$$

The terms A_1, A_2, D_1 and D_2 arise from the successive applications of (32) and (33). Combining equations (34), (35), (36) and (37), leads to the following expression for the support bending moment, including second order effects:

$$M^{II} = M(0) = \frac{WhA_2(n-1/2)}{\sqrt{n}a_n hA_1(1-nF/2S)} + Whn(D_2 - \frac{A_2 D_1}{A_1}) \quad (38)$$

Considering (25), the term $a_n h$ present in equation (38) may be put into the form:

$$a_n h = \sqrt{(F/S)/(\overline{K}(1-nF/2S)} \quad (39)$$

where

$$\overline{K} = EJ/Sh^2 \quad (40)$$

In its turn, the terms $a_i h$ and $a_{i+1}h$, mentioned several times along this work, will have expressions similar to (39), just replacing the quotient $nF/2S$ by iF/S or $(i+1)F/S$, respectively. On the other hand, the support bending moment, including only first order effects, is given by:

$$M^I = -Wh\left(n/2 + \sum_{i=1}^{n-1} i\right) \quad (41)$$

In order to verify the exemption of second order effects consideration, the 10% increase criterion, mentioned in subsection 1.1, will be applied for the support bending moment, with the modules of M^I and M^{II} given respectively by (41) and (38) (with changed signs, since these equations generate negative values for both the moments). Furthermore, according to the item 11.7.1 of ABNT NBR6118:2014 code, the loads W and F of equations (38), (39) and (41) must be multiplied by 1.4, seeing that this criterion is applied for the ultimate state. Consequently:

$$\frac{-1.4WhA_2(n-1/2)}{\sqrt{n}a_n hA_1(1-1.4nF/2S)} - 1.4Whn\left(D_2 - \frac{A_2 D_1}{A_1}\right) \leq 1.1 \times 1.4\, Wh\left(n/2 + \sum_{i=1}^{n-1} i\right) \quad (42)$$

It is implied that the term $a_n h$, present in equation (38), will have been obtained, applying (39) with $1.4F$ in place of F. The same change should be done in determining the terms $a_i h$ and $a_{i+1}h$ present in equations (28), (31), (32) and (33), with the purpose of obtaining A_1, A_2, D_1 and D_2. Performing the required algebraic transformations, inequality (42) changes to:

$$\frac{-A_2(n-1/2)}{\sqrt{n}a_n hA_1(1-1.4nF/2S)} - n(D_2 - \frac{A_2 D_1}{A_1}) \leq 1.1\left(n/2 + \sum_{i=1}^{n-1} i\right) \quad (43)$$

4.3 Determination of α_1

For a small number of floors, it is feasible to derive expressions of A_1, A_2, D_1 and D_2 as functions of F/S and then to replace them into the left member of (43). Thereafter, inequality (43) can be solved by trials, obtaining F/S. However, for a greater number of floors, it is necessary to apply equations (32) and (33) many times, leading to very long expressions for A_1 and A_2, causing the procedure to be impracticable.

In face of this circumstance, an alternative method was developed in order to determine F/S for buildings with any number of floors. Through this method, the solution is also obtained by means of trials. However, instead of deducing longer and longer expressions for A_1, A_2, D_1 and D_2, successive trials are done, assigning an initial value to F/S and determining numerical values for those variables. In each trial, the abovementioned formulary is applied in such a way to obtain numerical values for the right and left members of inequality (43). When these values result close enough to be considered identical, then the quotient F/S will have been determined. Furthermore, in order to apply this method, the value of $\overline{K}$, given by (40), must be defined.

Due to the great quantity of calculations, the method is computer aid. With the purpose of illustration, figure 4 shows a flow chart with the sequence of operations for determining F/S by means of trials. Representing by b the solution of inequality (43) obtained by

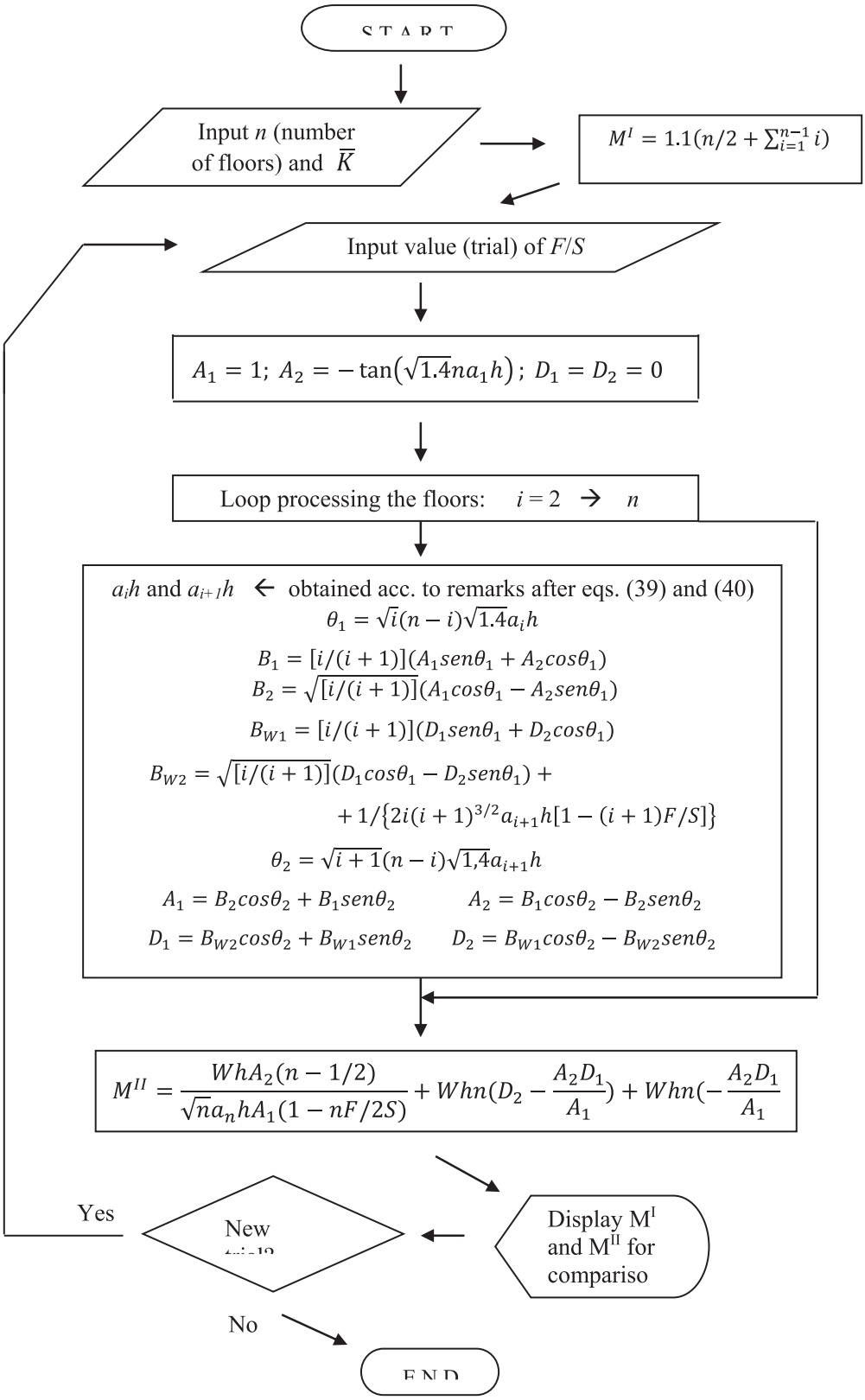

Figure 4
Sequence of operations for the solution of inequality (43)

Table 1
Values of α_1 independent of $\overline{K}$

Number of floors	α_1
1	0.42
2	0.47
3	0.49
≥ 200	0.65

this method and introducing successively equations (40) and (17), it may be written:

$$\frac{F}{S} = \frac{F\ell^2}{EI(2N + n^2/\overline{K})} \leq b \quad (44)$$

It can be observed in figure 3 that $\ell = H_{tot}/n$ and $F = N_k/n$, with N_k as defined in subsection 1.1. In its turn, the physical nonlinearity may be considered, replacing EJ by $(EI)_{sec}$ given by (7). Introducing these relations into inequality (44) and extracting the square root of both the members, results:

$$H_{tot}\sqrt{N_k/E_{CS}I_C}/\sqrt{0.5755n(2N + n^2/\overline{K}/r} \leq \sqrt{b} \quad (45)$$

Comparing (45) with equations (1) and (2) leads the limit α_1 of the instability parameter to be expressed by:

$$\alpha_1 = \sqrt{0.5755bn(2N + n^2/\overline{K}/r} \quad (46)$$

Therefore, introducing the desired number of floors (n) into the sequence of operations of figure 4, determines b; then, the limit coefficient α_1 can be obtained, applying equation (46). This was done for a series of floors quantities and for several values of $\overline{K}$. A concrete strength f_{ck} = 20 MPa was considered for effect of study, leading to r = 0.85, according to equation (3). Consequently, the ratio $(EI)_{sec}/E_{CS}I_C$ gives 0.677.
It was verified that, for less than four and more than 200 floors, the variation of α_1 in function of $\overline{K}$ is negligible. Thus, these values of

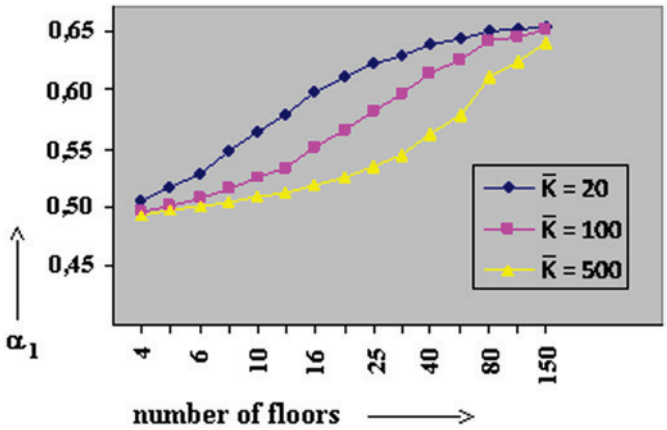

Figure 5
Graphs α_1 x number of floors

α_1, that may be considered independent of $\overline{K}$, are presented on table 1. For more than three and less than 200 floors, α_1 changes with $\overline{K}$. Table 2 shows a summary of the research results, where every column contains α_1 values relative to a fixed value of $\overline{K}$. In

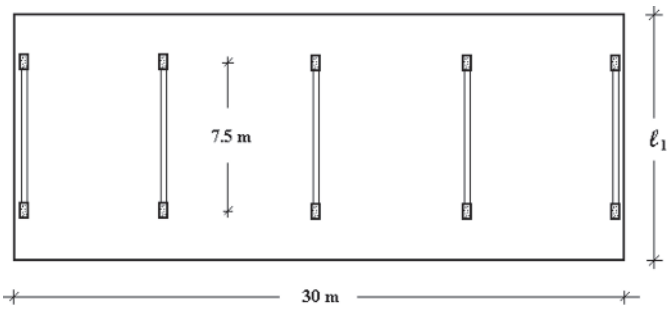

Figure 6
Transversal bracing system: examples 1, 3, 5, 7 and 9

Table 2
Values of α_1, varying $\overline{K}$ and the number of floors

Number of floors	Values of $\overline{K}$									
	500	300	250	200	150	100	80	60	40	20
4	0.493	0.494	0.494	0.494	0.495	0.496	0.497	0.498	0.500	0.506
5	0.498	0.499	0.499	0.499	0.500	0.502	0.503	0.505	0.509	0.518
6	0.501	0.502	0.503	0.503	0.505	0.507	0.509	0.512	0.516	0.528
8	0.505	0.507	0.508	0.510	0.512	0.516	0.519	0.523	0.531	0.548
10	0.509	0.512	0.513	0.516	0.519	0.525	0.529	0.535	0.545	0.564
12	0.512	0.516	0.518	0.521	0.526	0.534	0.539	0.546	0.557	0.578
16	0.519	0.526	0.529	0.533	0.540	0.551	0.557	0.566	0.579	0.598
20	0.526	0.535	0.540	0.545	0.553	0.566	0.573	0.582	0.595	0.611
25	0.535	0.548	0.553	0.560	0.569	0.582	0.590	0.598	0.609	0.622
30	0.544	0.559	0.565	0.573	0.582	0.596	0.602	0.610	0.619	0.629
40	0.563	0.580	0.586	0.594	0.603	0.614	0.619	0.624	0.631	0.638
50	0.579	0.596	0.602	0.609	0.616	0.625	0.629	0.633	0.637	0.642
100	0.623	0.633	0.636	0.639	0.642	0.645	0.646	0.647	0.649	0.650
150	0.639	0.644	0.645	0.647	0.648	0.650	0.650	0.651	0.652	0.652

Table 3
General information about examples 1 to 10

Example	1	2	3	4	5	6	7	8	9	10
N. of floors	5	5	10	10	20	20	30	30	50	50
Height (m)	15	15	30	30	60	60	90	90	150	150
N. of frames	3	3	5	3	5	5	9	7	13	11
Spacing (m)	10	7.5	7.5	7.5	7.5	4	3.75	5	2.5	3
N. of bays	1	3	1	3	1	3	1	3	1	3
Dimension l_1 (m)	12	16	12	16	12	18	12	23	20	23
Dimension l_2 (m)	–	10	–	10	–	12	–	17	–	17

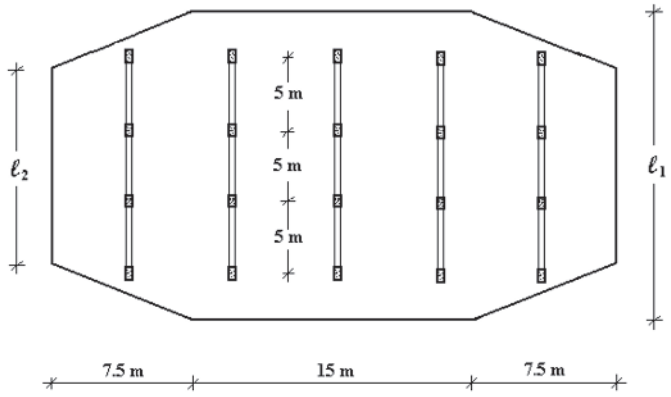

Figure 7
Transversal bracing system: examples 2, 4, 6, 8 and 10

order to cause this exposition to be not so long, the α_1 values are presented for a series of floors quantities that represents the just mentioned interval. In its turn, the set of $\overline{K}$ values written on table 2 represents the interval that includes the values of $\overline{K}$ found in the examples described in the next section.

5. Examples

5.1 Description of the tests

The plan of figure 6 shows the basic configuration of the transversal bracing system of a rectangular on plane building; it is composed by rigid frames spanning over a single bay of 7.5 m. In the same way, figure 7 shows the basic configuration of the transversal bracing system of a building with an oblong octagonal shape on plane; it is also composed by rigid frames which, in this case, span over three equal bays of 5 m. In both the cases, the frames are uniformly spaced and the spans are measured between column axes; the bearing elements are not represented. Each of these systems was employed in buildings having 5, 10, 20, 30 and 50 floors with a 3 m height, originating examples 1 to 10, whose general information is mentioned on table 3.

A concrete with f_{ck} = 40 MPa and basalt gravel was adopted, resulting in an elasticity modulus E_{CS} = 38 000 MPa. A total vertical load of 10 kN/m² per floor (characteristic value) was considered. A wind pressure of 1.5 kN/m² (characteristic value), constant along the building height, was adopted, since it was an experience with a formulation based on a model with uniform wind load.

Each of the 10 bracing systems was tested, aiming to determine the relation between vertical loads and horizontal stiffness that would result in a 10 % increase on the global bending moment at building support, concerning to the first order analysis; in this way, the limit a_1 of the instability parameter was determined. The procedure applied in each test consisted in assigning initial dimensions to the frame members cross sections and performing a second order analysis, employing the P-Delta method with double precision processing. Due to the bracing double symmetry in plane, the analyses were performed using a model composed by the transversal frames arranged in the same plane and joined among themselves by hinged bars.

After, this second order analysis was successively repeated, adjusting the cross section dimensions until achieve the desired 10% increase on the support global moment. Table 4 shows the cross section dimensions determined by this procedure.Rectangular sections were adopted for all the frame members, except the beams of examples 9 and 10, whose cross sections are T-shaped. Although being inadequate for the examples with a great floors number, the bracing systems consisting of single-bay and three-bay frames were preserved for the purpose of comparison.

Determining the instability parameter by means of equation (1) requires the previous evaluation of the moment of inertia I_c of a column equivalent to the transversal frames assemblage. This was done performing the procedure prescribed by item 15.5.2 of ABNT

Table 4
Cross sections dimensions (cm)

Example	Beams	Columns
1	25 x 68	25 x 47
2	19 x 47	19 x 47
3	25 x 68	25 x 68
4	20 x 60	20 x 60
5	40 x 76	40 x 100
6	23 x 60	30 x 89
7	33 x 78	40 x 130
8	29 x 65	29 x 117
9	64 x 193	64 x 130
	+ edges 45 x 12	
10	32 x 125	32 x 82
	+ edges 30 x 12	

Table 5
Inertia parameters of the examples

Example	I_C (m⁴)	$\overline{K}$	$(EI)_{sec} / E_{CS}I_C$
1	0.422	169	0.687
2	0.517	456	0.670
3	3.268	173	0.650
4	3.952	280	0.673
5	22.17	175	0.700
6	35.15	449	0.641
7	66.81	244	0.727
8	133.4	375	0.696
9	299.7	19.5	0.986
10	342.5	69.5	0.967

NBR 6118:2014 code. Thus, the equivalent inertia was determined for each example, by means of comparison between the top horizontal displacements resulting from linear analyses of the bracing system and the equivalent column under wind loading. The I_C values determined by this procedure are presented on table 5. The coefficient $\overline{K}$ of each example was evaluated applying equation (40), with *J* and *S* determined as explained in section 3. The values of $\overline{K}$ are also presented on table 5.

The physical nonlinearity was considered by means of the individual members stiffness reduction, expressed by equations (5) and (6). Besides applying *P*-Δ method, a physical nonlinear analysis of each bracing system subject exclusively to wind loading was performed; it in fact consists of a linear analysis with the just mentioned members stiffness reduction. Afterwards, the $(EI)_{sec} / E_{CS}I_C$ relation of the frame members assemblage of each example was determined, comparing the top horizontal displacements resulting from the analysis with the members stiffness reduction and from the one without this reduction. The values of this relation are written on last column of table 5.

5.2 Results discussion

Tables 1 and 2 show values of the α_1 limit coefficient, computed by means of the operations sequence of figure 4, followed by application of equation (46). In its turn, figure 5 shows graphs representing the variation of α_1 with the number of floors, for three different values of $\overline{K}$. It can be observed that the values of α_1 increase with the floors number, varying from 0.42 (one floor) until 0.655 (for the floors number tending to infinite). Nevertheless, as was emphasized at the end of section 4, these values were evaluated for a relation $(EI)_{sec} / E_{CS}I_C = 0.677$; changing it, the α_1 values will change proportionally to its square root.

Table 2 and figure 5 also show that, for the same number of floors, α_1 increases as $\overline{K}$ decreases, in other words, as the frames bending stiffness decreases in relation to the shear stiffness and, therefore, as the frames bending flexibleness increases in relation to the shear flexibleness. This is because a greater bending flexibleness tends to induce a deflected shape with significant horizontal displacements occurring only in the building upper region; on the contrary, in a structure more flexible to shear, considerable horizontal displacements occur directly from the building lower region. The decrease of the number of floors with significant horizontal displacements causes the global bending moment portion due to second order effects to decrease, inducing an increase of the α_1 limit coefficient.

The graphs of figure 5 show that the variation of α_1 with $\overline{K}$ is more accentuated in an intermediate interval of the floors number. For example, for 25 floors, the difference between the values of α_1 regarding to $\overline{K}$ equal to 20 and to 500 is 16%, corresponding to a difference of 35% between the respective vertical load/horizontal stiffness ratios.

In its turn, the values of α obtained in the examples are presented on second column of table 6. It can be verified that they also increase with the floors number. For the same number of floors, the values of α relative to the single-bay examples tend to be greater than the three-bay ones, while the contrary occurs with the values of $\overline{K}$, as is written on table 5. This is coherent with that was previously explained, since in the single-bay frames the axial deformation on the columns tends to be greater, because of the lower quantity of them, leading to greater deflections due to global bending.

The third column of table 6 shows predictions of α_1 resulting from interpolation of table 2 values, entering the floors number and the $\overline{K}$ coefficient of each example. It was verified that these predictions present, in some cases, expressive discrepancies in relation to the α values found in the examples.

Afterwards, the predicted α_1 values were recomputed, changing the factor 0.5755/*r* of equations (7) and (46) by the relations $(EI)_{sec} / E_{CS}I_C$ mentioned on table 5. These recomputed α_1 values, as well as the differences between them and the α values found in the examples are presented on fourth and fifth columns of table 6, respectively. It can be observed that these differences are lesser than 1 % for all the examples. Figures 8 (single-bay examples) and 9 (three-bay examples) show graphically the good accuracy degree achieved on predicting the values of α_1.

The need of recalculating α_1 in function of the $(EI)_{sec} / E_{CS}I_C$ factors was mainly due to the difference between the value of f_{ck} considered in the computation of tables 1 and 2 (20 MPa) and the one adopted in the examples (40 MPa). Therefore, this difference was a determinant factor for concluding that it is necessary to evaluate the physical nonlinearity accurately, in order to reach a good

Table 6
Values of α_1 resulting from the research

Example	α [1]	α_1 [2]	α_1 [3]	Difference [4]
1	0.503	0.500	0.503	0
2	0.499	0.498	0.496	0.60%
3	0.511	0.518	0.508	0.59%
4	0.511	0.512	0.511	0
5	0.555	0.549	0.558	0.54%
6	0.517	0.528	0.514	0.58%
7	0.587	0.566	0.587	0
8	0.556	0.553	0.561	0.90%
9	0.770	0.642	0.775	0.65%
10	0.747	0.631	0.754	0.94%

[1] Values found in the examples;
[2] values predicted from table 2;
[3] α_1 (2) with $(EI)_{sec} / E_{CS}I_C$ factor improvement;
[4] Differences between α^1 and α_1^3.

degree of precision in the prediction of the α_1 limit of a building with a given number of floors and a $\overline{K}$ stiffness ratio.

It can also be observed that the values of α obtained in the examples vary from a minimum of 0.499 in example 2 until a maximum of 0.770 in example 9. The proportion between these extreme values is close to 1.5:1. Since their computation includes a square root extraction, the proportion between the radicands (vertical load/horizontal stiffness relations) associated to these extreme values is higher than 2:1.

The extent of this variability shows the importance of having a way of predicting a limit α_1 appropriated to the floors number and the $\overline{K}$ ratio of a given building to be designed, in place of the fixed values prescribed by the ABNT NBR 6118:2014 code. For example, regarding to the fixed value 0.5 (prescribed for more than three floors), table 2 gives values ranging from 0.493 (four floors and $\overline{K}$ = 500) until 0.652 (150 floors and $\overline{K}$ = 40 or 20). These values were obtained for a constant relation $(EI)_{sec} / E_{CS}I_C$ = 0.5755/*r*. Determining this relation for each case, α_1 can achieve greater values further, as was verified in the examples.

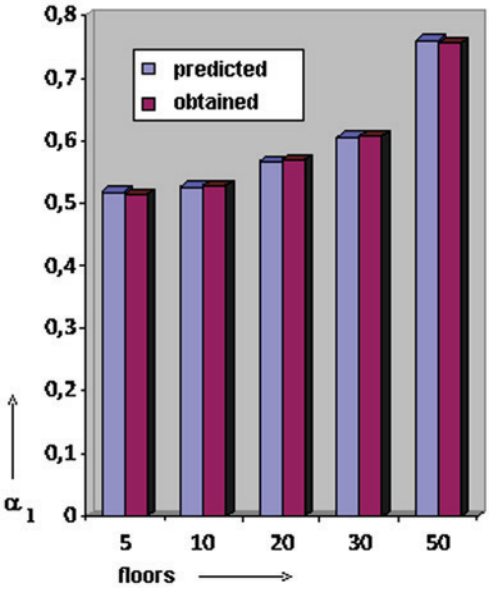

Figure 8
Values of α_1: single-bay examples

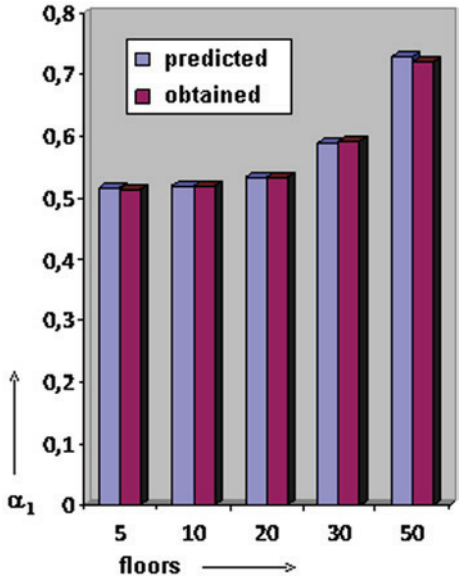

Figure 9
Values of α_1: three-bay examples

6. Conclusions

In the present work, a method based on the Beck and König discrete model (Figure 1) was developed, considering equally spaced floors and uniform wind load. The method consists in solving inequality (43) by means of trials and then to input its solution into equation (46), obtaining α_1. Since the method is computer aid, α_1 can be obtained for any number of floors and any value of $\overline{K}$, as can be seen in tables 1 and 2.

A study concerning bracing systems composed exclusively by walls and/or cores, performed by Ellwanger [2], deduced expressions for predicting the α_1 limit that depend only of the floors number. In its turn, the framed systems, treated in this work, require the previous definition of two additional parameters in order to determine α_1.

The first of these parameters is the relation $\overline{K}$ between the system bending and shear stiffness, expressed by equation (40), being *J* and *S* determined as explained in section 3. The second parameter is the relation $(EI)_{sec} / E_{CS}I_C$ of the bracing system (influence of physical nonlinearity). A way to obtain it is to perform another linear analysis, considering the cross sections reduction expressed by equations (4) to (6). The relation $(EI)_{sec} / E_{CS}I_C$ is then determined through the comparison between the system top horizontal displacements resulting from the analyses with the reduced cross sections and with the non-reduced ones.

A topic for continuity of research in this subject is to investigate the viability of fixing lower limits of the relation $(EI)_{sec} / E_{CS}I_C$ for particular cases (intervals of floors numbers, number of bays, building height/width relation, equality or inequality between A_s and A_s' beam reinforcement areas etc.) and introducing them into equation (46), through the change of factor 0.5755/*r*. In this way, the structural designer could decide to analyze the structure with the reduced cross sections or simply to adopt the just mentioned estimation of $(EI)_{sec} / E_{CS}I_C$.

In the study concerning wall- or core-braced systems, Ellwanger [2] dealt with uniform wind loading as well as wind loads varying according to the prescriptions of the ABNT NBR 6123:1988 code (Buildings Wind Loads, ABNT[11]). It was verified that the α_1 values computed for these loading patterns are very close, with differences lower than 1.7%. Hence, this work didn't deal with variable wind load. However, on following the research in this topic, it is advisable to check if the α_1 values of framed systems are also close for the two wind loading patterns.

The good accuracy attained by the method proposed by Ellwanger [2] and by the present study recommends its adoption in the research of procedures for determining the limit α_1 of wall-frame and core-frame bracing systems. Cases of unequally spaced floors and horizontal stiffness varying along the building height can also be

considered. Another topic of searching may be the feasibility of deriving interpolation functions that reproduce the values sequences of tables 1 and 2. It must be emphasized that all of this has to be done in such a manner to keep the formulation simplicity, just one of the greater advantages of using the instability parameter.
It must be accentuated that the results obtained in this work refer to structural systems consisting of repetitive and equally spaced rigid frames. In order to the instability parameter with a variable limit to be introduced into the structures design practice, it is necessary the method developed in this work to be checked by a much more diversified series of examples, including non uniform frames as well as irregular arrangements of frames. Furthermore, it is recommended that a more realistic analysis model will be adopted for the tests, modeling the structure as a three-dimensional frame, considering the floors behaving as rigid diaphragms.

7. References

[1] Ellwanger, R.J.; Um limite variável para o parâmetro de instabilidade de estruturas de contraventamento formadas por associações de pórticos com paredes ou núcleos. *In*: Revista IBRACON de Estruturas e Materiais, vol. 5, nº 1, pp. 120-136 , São Paulo, 2012.

[2] Ellwanger, R.J.; Floors number influence on the instability parameter of reinforced concrete wall- or core-braced buildings. *In*: Revista IBRACON de Estruturas e Materiais, vol. 6, nº 5, pp. 797-810 , São Paulo, 2013.

[3] ABNT – Associação Brasileira de Normas Técnicas; NBR 6118 – Projeto de Estruturas de Concreto – Procedimento, Rio de Janeiro, 2014.

[4] Franco, M. and Vasconcelos, A.C.; Practical Assessment of Second Order Effects in Tall Buildings. *In*: Colóquio do CEB-FIP Model Code 1990, pp. 307-24, Rio de Janeiro, 1991.

[5] Alves, E.C. e Feitosa, L.A.; Estudo da estabilidade global de edifícios altos com lajes protendidas. *In*: Revista IBRACON de Estruturas e Materiais, vol. 8, nº 2, pp. 164-195, São-Paulo, 2015.

[6] Cicolin, L.A.B. e Figueiredo Filho, J.R.; Estabilidade em edifícios de concreto armado com lajes sem vigas: influência de pórticos formados por faixas de lajes e vigas invertidas nas bordas. *In*: Revista IBRACON de Estruturas e Materiais, vol. 4, nº 3, pp. 481-500, São Paulo, 2011.

[7] Freitas, F.C., Luchi, L.A.R. e Ferreira, W.G.; Análise da estabilidade global das estruturas e ações de controle dos seus efeitos. *In*: Revista IBRACON de Estruturas e Materiais, vol. 9, nº 2, pp. 153-191, São Paulo, 2016.

[8] Pinto, R.S. e Ramalho, M.A.; Inércia equivalente das estruturas de contraventamento de edifícios em concreto armado. *In*: Cadernos de Engenharia de Estruturas, São Carlos, v. 9, n° 38, p. 107-136, 2007.

[9] Taranath, B.S.; Reinforced Concrete Design of Tall Buildings, Boca Raton, CRC Press, 2010.

[10] Stafford Smith, B. and Coull, A.; Tall Building Structures: Analysis and Design, New York, John Wiley & Sons Inc., 1991.

[11] ABNT – Associação Brasileira de Normas Técnicas; NBR 6123 – Forças Devidas ao Vento em Edificações, Rio de Janeiro, 1988.